Published in final edited form as:
Alzheimer Dis Assoc Disord. 2012 April ; 26(2): 186–190. doi:10.1097/WAD.0b013e31822de18c.

Anomalous PiB enhancement in the Superior Sagittal and Transverse Venous Sinuses

Scott B. Raymond, PhD[*], **Ann D. Cohen, PhD**[†], **Carl Becker, PhD**[‡], **Julie Price, PhD**[‡], and **William E. Klunk, MD, PhD**[†]

[*]The Harvard-MIT Division of Health Sciences and Technology, Cambridge, MA

[†]Department of Psychiatry, University of Pittsburgh School of Medicine, Pittsburgh, PA

[‡]Department of Radiology, University of Pittsburgh School of Medicine, Pittsburgh, PA

Abstract

Pittsburgh compound-B (PiB), an amyloid-binding positron emission tomography (PET) tracer, is widely used for imaging amyloid-β in those with and at risk for Alzheimer disease. Here, we report on an otherwise normal 68-year-old female with abnormally high and very focal PiB retention. Coregistered T1-weighted magnetic resonance imaging and dynamic 2-fluoro-2-deoxy-D-glucose (FDG) images confirmed that the focal PiB enhancement was in the superior sagittal and transverse sinuses, outside of the adjacent cortex. Flow through the venous vasculature was normal as assessed by dynamic FDG PET imaging. These features supported the conclusion that PiB retention was not simply due to a hemodynamic abnormality, but may have represented PiB binding to fibrillar deposits of a β-sheet protein (ie, amyloid), whose nature is currently unclear.

Keywords

amyloid-β; PET imaging; Alzheimer disease; PIB; FDG

Pittsburgh compound-B (PiB) is a positron emission tomography (PET) tracer that binds amyloid-β deposits with high specificity, enabling PET imaging of amyloid aggregates in Alzheimer disease (AD) patients.[1,2] PiB is a powerful tool for studying AD and has been used for a wide range of clinical and basic disease research.[3] Since the first human PiB scans in 2002, several thousands of patients have received PiB imaging at more than 50 centers around the world. PiB is currently used to monitor therapy in a number of clinical trials[4,5] and may eventually see clinical use to help diagnose dementia.[2,6–9] Further, recent advances in F^{18}-labeled amyloid imaging agents such as Amyvid,[10] Flutemetamol,[11], and Florbetaben[12] have made amyloid imaging more accessible due to the longer half-life of F^{18}, making the transport of these compounds to remote PET imaging sites possible. As amyloid imaging becomes more widespread, it is important to document and study amyloid imaging variants. Here, we describe an otherwise normal individual with unusual PiB retention in the venous sinuses.

Reprints: William E. Klunk, MD, PhD, Western Psychiatric Institute and Clinic, Room 1422 TDH, 3811 O'Hara Street, Pittsburgh, PA 15213-2593 (klunkwe@upmc.edu).

GE Healthcare holds a license agreement with the University of Pittsburgh based on the technology described in this article. Dr. Klunk is a coinventor of PiB and, as such, has a financial interest in this license agreement. GE Healthcare provided no grant support for this study and had no role in the design or the interpretation of the results or the preparation of this manuscript. All other authors have no conflicts of interest with this study and had full access to all of the data in the study and take responsibility for the integrity of the data and the accuracy of the data analysis.

METHODS

Imaging

PiB and 2-fluoro-2-deoxy-D-glucose (FDG) PET and structural magnetic resonance imaging (MRI) studies were performed as described previously in detail.[13,14] MR images were acquired on a 1.5 T scanner using a spoiled gradient recall sequence and coregistered with PET images using automated methods.[15,16]

Image Analysis

Region-of-interest-based analyses and PiB(−) case definitions were performed as described previously.[7,13,14,17] Volumes of interest (VOIs) for the venous sinuses and internal carotids were determined using the initial "wash-in" frames ($t = 0$ to 2 min) on FDG scans. We defined the venous sinus VOIs using an oval (16.52mm^2) drawn in 5 consecutive slices (2.46mm per slice) centered at the confluence of the superior sagittal sinus and the transverse sinuses. Carotid VOIs were drawn bilaterally with an oval (24.26 cm^2) on 5 slices spanning the cavernous segment of the internal carotid. Subgenual anterior cingulate and precuneus VOIs were generated in a previous study.[13]

Venous anatomy was assessed using the $t = 45$ seconds acquisition from the dynamic FDG scan, which approximates the venous phase. At this time point, FDG is primarily pooling in the venous circulation, allowing clear visualization of the venous anatomy. Raw FDG images were median filtered and thresholded to remove noise.

RESULTS

The patient, referred to hereafter as C49, was a 68-year-old female with an unremarkable medical history. She was evaluated with the standard neurological, psychiatric, and neuropsychological examinations used at the University of Pittsburgh Alzheimer Disease Research Center (ADRC) as described previously.[7,13,18] All participants provided informed consent for both the ADRC clinical examination and the PET imaging protocol. This study was approved by the Human Use Subcommittee of the Radio-active Drug Research Committees and the Institutional Review Board of the University of Pittsburgh.

C49 was enrolled as a cognitively normal control. Five other cognitively normal controls with no PiB retention [ie, PiB negative (−) controls] were used for comparison in the following analysis. C49 received identical assessments and imaging at a 12-month follow-up study.

Imaging

MRI scans were normal as read by an experienced radiologist. On PiB PET scans, C49 exhibited enhancement in the venous sinuses, beginning in the superior sagittal sinus at the level of the superior parietal lobe, descending to the confluence of the sinuses, and continuing laterally along both transverse sinuses (Fig. 1). The straight sinus did not exhibit PiB enhancement. Localization to the venous sinuses was confirmed by T1-weighted MRI (Fig. 1, top row) and by the venous phase of a dynamic FDG scan (Fig. 2). When overlaid on the MRI, the PiB signal at the superior sagittal sinus and the sinus confluence overlapped slightly with adjacent cortex, likely a result of the point-spread function of PET reconstruction (approximately 6mm full width at half maximum).[15,16,19] PiB retention in all other brain regions was negligible. The 1-year follow-up PiB imaging study in C49 showed similar PiB retention in the venous sinuses (not shown).

We quantified these observations by comparing PiB standardized uptake values (SUVs) in C49 (n = 2, baseline scan and 1 y rescan) and PiB(−) control scans (n = 5) for VOIs including the venous sinuses, internal carotids, subgenual anterior cingulate cortex, and precuneus cortex. The venous sinus PiB SUV was higher in C49 compared with the controls at late time-points (Fig. 3A). When normalized to the carotid arteries, which approximate the vascular input function and control for dosage and hemodynamic differences between participants, the C49 sinus PiB SUV was 25% to 46% greater than the controls at late time points (Fig. 3B). Other brain regions that are often the first to show increased PiB retention in PiB(+) controls, such as the subgenual anterior cingulate and the precuneus cortex, did not retain PiB in C49 or PiB(−) controls (data not shown). In summary, C49 exhibited focal PiB retention in the venous sinuses, with otherwise normal PiB retention throughout the brain.

We hypothesized that an apparent increase in venous sinus PiB retention in C49 could be an artifact of hemodynamic abnormalities in the sinus. In that case, the pharmacokinetics of other tracers should be similarly affected. We thus compared the PiB PET findings with those obtained during a 2-fluoro-2-deoxy-D-glucose study. FDG, a glucose analog, normally distributes quickly (<1 min) and accumulates only in metabolically active cells; the FDG signal in vascular structures, such as the carotids, normally decreases rapidly to baseline after the intravenous bolus.

Sinus FDG in C49 decreased quickly after intravenous administration compared with sinus PiB, which cleared relatively slowly (see Figs. 3A, C). C49 sinus FDG kinetics were similar to, if not slightly faster than, sinus FDG kinetics in PiB(−) controls (Figs. 3C, D). In contrast, sinus PiB in C49 washed out more slowly than PiB(−) controls and seemed to plateau at late times (eg, 60 to 90 min, Figs. 3A, B).

DISCUSSION

We observed anomalous PiB retention in the venous sinuses of a cognitively normal individual. PiB distribution volume ratio was abnormally high in the superior sagittal and transverse sinuses, but was typical of other PiB(−) controls in other regions of the brain. When overlaid on the MR image, PiB enhancement was clearly associated with dural structures outside of the brain parenchyma (Fig. 1, bottom row).

In this case, sinus PiB enhancement did not seem to be the result of a hemodynamic abnormality, because another tracer, FDG, was not retained abnormally in the sinuses. In fact, the sinus FDG signal in our participants was lower than the PiB(−) controls for later time-points, suggesting more complete vascular clearance (Fig. 3C). It should be noted that sinus FDG was, in some patients, partially contaminated from surrounding cortical structures because of VOI placement and reconstruction constraints, and therefore increased at later time-points(> 10min) (Figs. 3C, D), PiB(−) controls).

These findings support the hypothesis that the abnormal PiB retention was caused by a β-sheet structured protein aggregate deposited in the walls of the venous sinuses. To our knowledge, there is no precedent for cerebral amyloid angiopathy in the venous sinuses, and this is the first venous sinus PiB enhancement seen at our institution after >300 subjects. It is unlikely that the PiB retention was the result of systemic amyloidosis, because our patient had no history of primary or secondary amyloidosis. Furthermore, to our knowledge, there is no record in the literature of systemic amyloidosis manifesting in the venous sinus. Finally, C49 had no history of B-cell lymphoma, a condition reported to be associated with the presence of amyloid in the dura.[20] Thus, if there is a PiB-enhancing amyloid deposit in the venous sinuses of this case, its identity remains uncertain.

This case provides multiple warnings about PiB imaging and analysis. First, when PiB enhancement occurs at the extreme edges of the brain, a coregistered MRI can be helpful for corroborating cortical versus extracortical signal. We have recently observed a small number of patients with the clinical diagnosis of mild cognitive impairment or early AD who exhibit focal PiB enhancement in the occipital pole. In such cases, care should be taken to distinguish cortical amyloid from deposits in the sinus and might be better informed using overlaid PET-MRI composite images.

Second, in studying this case, we discovered that the image processing protocol used to generate parametric images from raw PET measurements sometimes obscured the PiB signal coming from areas outside of the brain boundaries. During our processing stream, the analyst draws a mask around the brain boundaries, as seen on the MRI, which is then used to suppress all PET signals outside of the brain in subsequent parametric images. In some cases, including the initial analysis of the 12-month rescan study of our patient, the mask excluded focal PiB enhancement in dural structures. Thus, we suspect that reassessment of imaging archives might uncover other cases of extracortical PiB retention.

In summary, we have described a PiB imaging variant with anomalous PiB enhancement in the venous sinuses that is apparently not a result of a hemodynamic abnormality. Care must be taken with PiB, and presumably other amyloid-imaging tracers, so as to not misread sinus retention as parenchymal retention.

Acknowledgments

The authors thank Dr Lisa Weissfeld for advice on stastical analysis and Dr James Mountz for reading the imaging studies.

Supported by the National Institutes of Health grants: P50 AG005133, R37 AG025516, and P01 AG025204. Scott Raymond was supported by T32 EB001680.

REFERENCES

1. Mathis CA, Bacskai BJ, Kajdasz ST, et al. A lipophilic thioflavin-T derivative for positron emission tomography (PET) Imaging of amyloid in brain. Bioorg Med Chem Lett. 2002; 12:295–298. [PubMed: 11814781]
2. Klunk WE, Engler H, Nordberg A, et al. Imaging brain amyloid in Alzheimer's disease with Pittsburgh Compound-B. Ann Neurol. 2004; 55:306–319. [PubMed: 14991808]
3. Klunk, WE.; Mathis, CA. Amyloid Imaging and (What is"Normal") Aging. In: Jagust, W.; D'Esposito, M., editors. Imaging the Aging Brain. New York: Oxford University Press; 2009.
4. Kadir A, Andreasen N, Almkvist O, et al. Effect of phenserine treatment on brain functional activity and amyloid in Alzheimer's disease. Ann Neurol. 2008; 63:621–631. [PubMed: 18300284]
5. Ryu EK, Chen X. Development of Alzheimer's disease imaging agents for clinical studies. Front Biosci. 2008; 13:777–789. [PubMed: 17981587]
6. Wolk DA, Klunk WE. Update on amyloid imaging: from healthy aging to Alzheimer's disease. Curr Neurol Neurosci Rep. 2009; 9:345–352. [PubMed: 19664363]
7. Aizenstein HJ, Nebes RD, Saxton JA, et al. Frequent amyloid deposition without significant cognitive impairment among the elderly. Arch Neurol. 2008; 65:1509–1517. [PubMed: 19001171]
8. Mikhno A, Devanand D, Pelton G, et al. Voxel-based analysis of 11C-PIB scans for diagnosing Alzheimer's disease. J Nucl Med. 2008; 49:1262–1269. [PubMed: 18632806]
9. Zhou Y, Resnick SM, Ye W, et al. Using a reference tissue model with spatial constraint to quantify [11C]Pittsburgh compound B PET for early diagnosis of Alzheimer's disease. Neuroimage. 2007; 36:298–312. [PubMed: 17449282]
10. Clark CM, Schneider JA, Bedell BJ, et al. Use of florbetapir-PET for imaging beta-amyloid pathology. JAMA. 2011; 305:275–283. [PubMed: 21245183]

11. Vandenberghe R, Van Laere K, Ivanoiu A, et al. 18F-flutemetamol amyloid imaging in Alzheimer disease and mild cognitive impairment: a phase 2 trial. Ann Neurol. 2010; 68:319–329. [PubMed: 20687209]
12. Barthel H, Gertz HJ, Dresel S, et al. Cerebral amyloid-beta PET with florbetaben ((1)F) in patients with Alzheimer's disease and healthy controls: a multicentre phase 2 diagnostic study. Lancet Neurol. 2011; 10:424–435. [PubMed: 21481640]
13. Price JC, Klunk WE, Lopresti BJ, et al. Kinetic modeling of amyloid binding in humans using PET imaging and Pittsburgh Compound-B. J Cereb Blood Flow Metab. 2005; 25:1528–1547. [PubMed: 15944649]
14. Lopresti BJ, Klunk WE, Mathis CA, et al. Simplified quantification of Pittsburgh compound B amyloid imaging PET studies: a comparative analysis. J Nucl Med. 2005; 46:1959–1972. [PubMed: 16330558]
15. Woods RP, Mazziotta JC, Cherry SR. MRI-PET registration with automated algorithm. J Comput Assist Tomogr. 1993; 17:536–546. [PubMed: 8331222]
16. Minoshima S, Koeppe RA, Mintun MA, et al. Automated detection of the intercommissural line for stereotactic localization of functional brain images. J Nucl Med. 1993; 34:322–329. [PubMed: 8429356]
17. Ziolko SK, Weissfeld LA, Klunk WE, et al. Evaluation of voxel-based methods for the statistical analysis of PIBPET amyloid imaging studies in Alzheimer's disease. Neuroimage. 2006; 33:94–102. [PubMed: 16905334]
18. Lopez O, Becker J, Klunk W, et al. Research evaluation and diagnosis of probable Alzheimer's disease over the last two decades: I. Neurology. 2000; 55:1854–1862. [PubMed: 11134385]
19. Meltzer C, Becker J, Price J, Moses-Kolko E. Positron emission tomography imaging of the aging brain. Neuroimaging Clin N Am. 2003; 13:759–767. [PubMed: 15024959]
20. Lehman NL, Horoupian DS, Warnke RA, et al. Dural marginal zone lymphoma with massive amyloid deposition: rare low-grade primary central nervous system B-cell lymphoma. Case report. J Neurosurg. 2002; 96:368–372. [PubMed: 11838814]

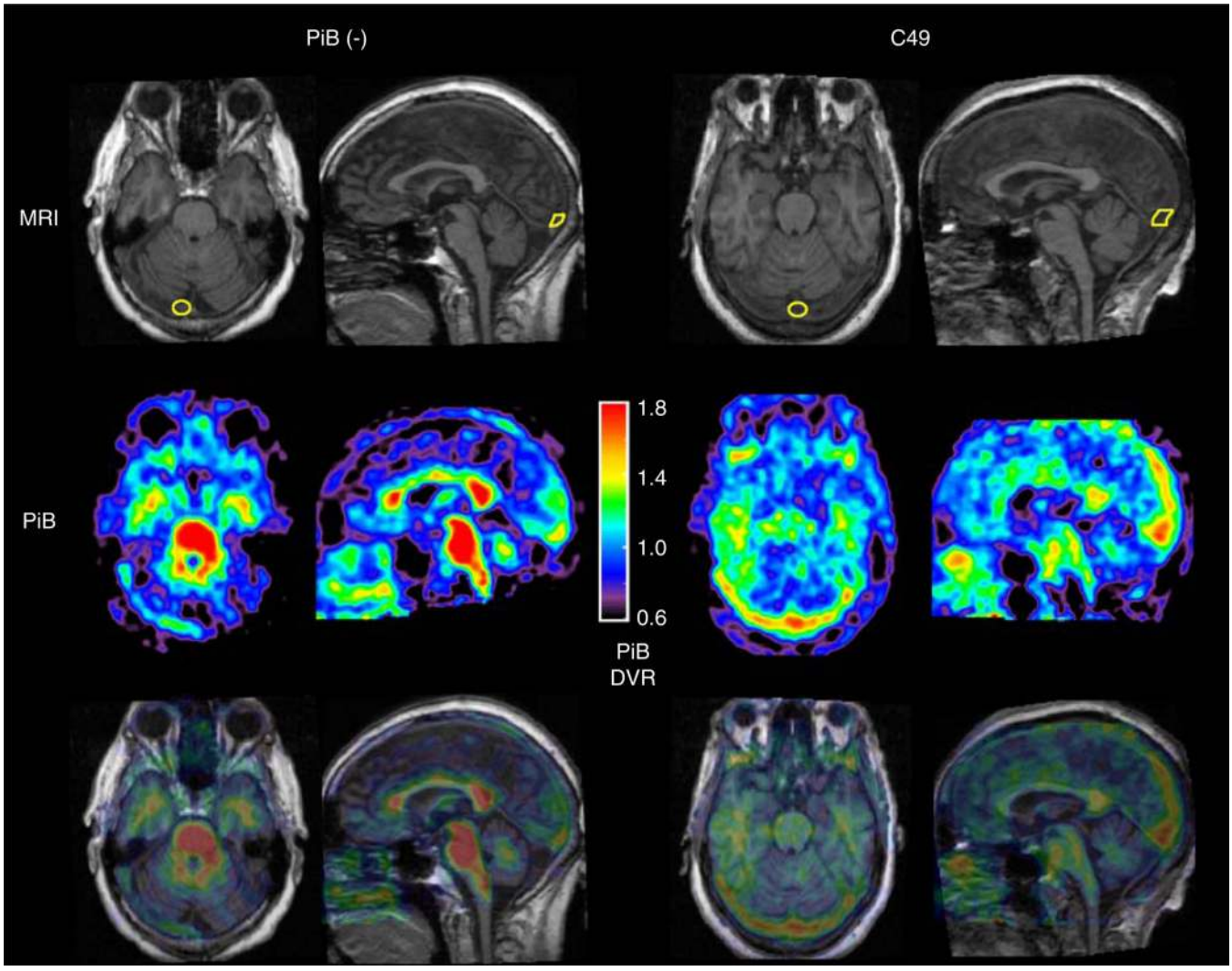

FIGURE 1.

Pittsburgh compound-B (PiB) distribution volume ratio (DVR) images with T1-weighted [spoiled gradient recall (spgr)] magnetic resonance imaging (MRI) for case C49 (right) and a stereotypical PiB(−) control (left). Axial slices (first and third columns) are taken at the sinus confluence; sagittal slices (second and fourth columns) are taken at the midline. First row: T1-weighted (spgr) MR images. Volumes-of-interest (VOIs) were established for the venous sinus using early time-frames from 2-fluoro-2-deoxy-D-glucose (FDG) images (not shown) and confirmed on coregistered MRI, shown in yellow. Second row: Logan parametric DVR images using the cerebellum ROI as reference. The DVR scale (0.6 to 1.8) is shown at the center. Third row: PiB DVR from the middle row overlaid on corresponding MRI slices.

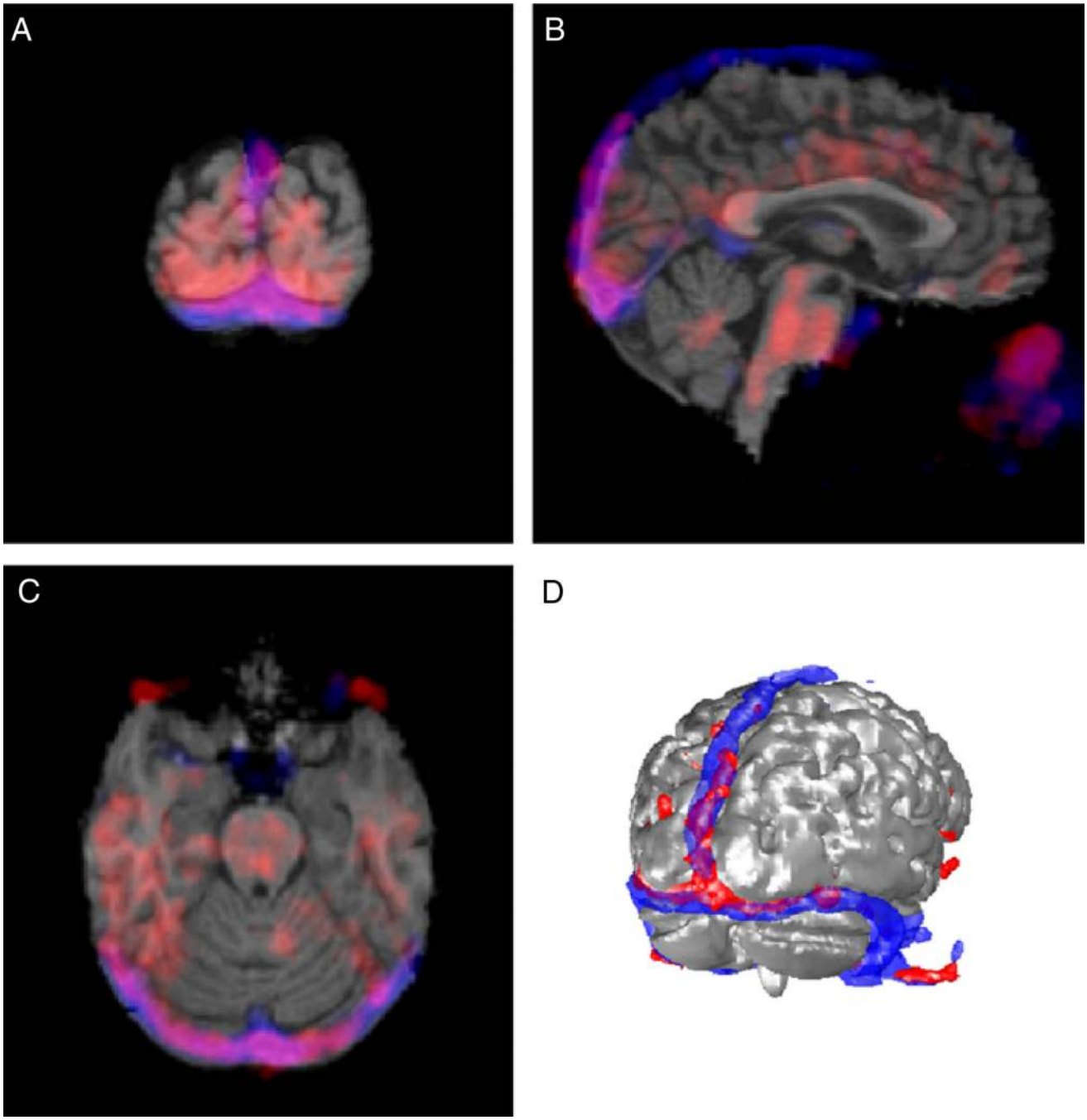

FIGURE 2.

The 2-fluoro-2-deoxy-D-glucose (FDG) venogram and Pittsburgh compound-B (PiB) enhancement. To confirm the localization of PiB enhancement to the venous sinuses, we used an FDG venogram, obtained from the $t = 45$ seconds frame of the dynamic FDG scan. The representative coronal (A), sagittal (B), and axial (C) slices through the torcular herophili are shown, with PiB distribution volume ratio (DVR) in red, the FDG venogram in blue, and the T1-weighted magnetic resonance imaging (MRI) shown in grayscale. PiB DVR images are thresholded from 1.1 to 1.3. A, Three-dimensional representation showing the cortical surface (gray, obtained from MRI), PiB (red), and FDG venogram (blue) shown

in (D). PiB DVR of 1.2 was used to calculate the red isosurface and FDG isosurface is at 37% of the maximum intensity.

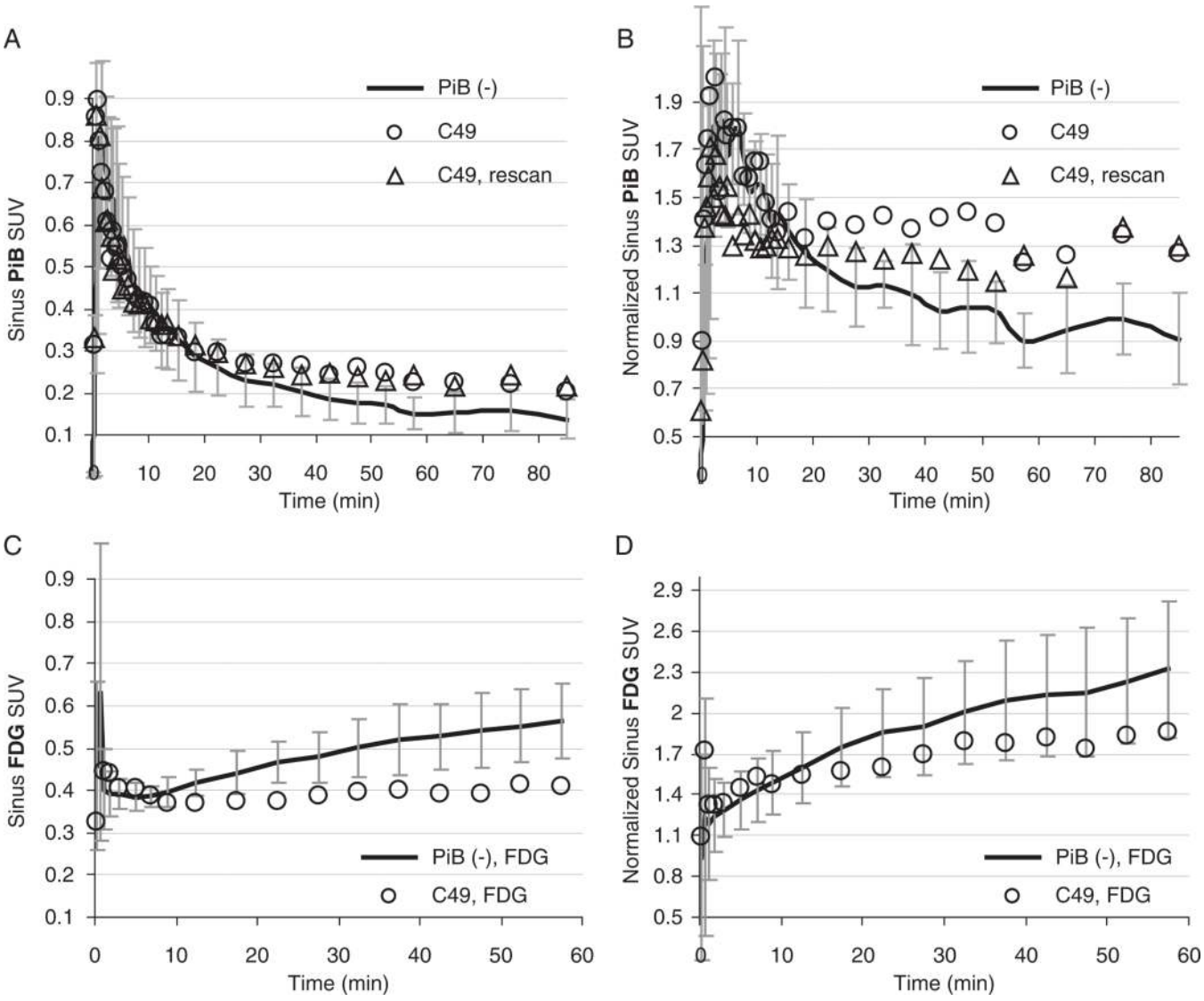

FIGURE 3.

Volume of interest (VOI) analysis of PiB and 2-fluoro-2-deoxy-D-glucose (FDG)-standardized uptake value (SUV) kinetics. SUV kinetics from C49 were compared with the controls for PiB and FDG scans in the venous sinus VOI. In all plots, controls are indicated with the solid line; error bars show the standard deviation [n = 5, PiB(−)]. A, Venous sinus VOI for C49 scan (circle) and 1-year rescan (triangle) compared with PiB(−) controls (solid line). B, Venous sinus VOI normalized to the carotids. C, Venous sinus FDG kinetics for the C49 baseline scan (circles) and PiB(−) controls (solid line). D, Venous sinus FDG kinetics normalized to the carotids.